Effect of Plasma Polymer Deposition Methods on Copper Corrosion Protection

Y. LIN and H. YASUDA*

Department of Chemical Engineering and Center for Surface Science and Plasma Technology, University of Missouri-Columbia, Columbia, Missouri 65211

SYNOPSIS

The behavior of plasma polymer coating for Cu corrosion protection was investigated in dc cathodic polymerization, with and without anode magnetron enhancement, af magnetron glow discharge polymerization, and rf glow discharge polymerization. The combination of visual and scanning electron microscopy observations established general trends in an accelerated wet/dry cycle corrosion testing environment containing 0.1*N* chloride ions. Dc anodic magnetron cathodic polymerization of TMS offered the best Cu corrosion protection due to an enhanced deposition uniformity and adhesion of the deposited plasma polymer to the Cu substrate. No corrosion was observed after 25 wet/dry cycle accelerated corrosion tests when uncoated Cu suffered a severely generalized attack in one cycle. Superior corrosion protection was also performed by an af plasma polymerized coating of $C_4F_{10} + H_2$ (1 : 1) at a low-energy input density and of methane at high-energy input and high deposition thickness carried out in the range of this study. The application of plasma polymers which showed high water vapor permeation resistance and surface dynamic stability greatly reduced the pitting densities. © 1996 John Wiley & Sons, Inc.

INTRODUCTION

Plasma polymerization is a highly system-dependent process. For a given monomer, the properties of a plasma polymer are closely related to the design factor of the reactor, the location of the substrate in the reactor, the frequency of the electric power source, and other factors. For metal substrates, cathodic glow discharge polymerization, in which a metal substrate was used as the cathode of the dc glow discharge, provides a distinctive advantage in which the deposition of plasma polymer occurs nearly exclusively onto the substrate surface.[1] Additionally, there seems to exit a general trend that the adhesion of a plasma polymer on a metal surface is highly dependent on the mode of plasma polymerization and that the adhesion follows a trend: (dc cathodic polymerization) > (af magnetron glow discharge polymerization) ≫ (rf glow discharge polymerization).[2] The present study was undertaken to investigate the effects of these three methods on the passivating or protecting of copper from corrosion.

Corrosion of copper has been the subject of great interest because of the numerous uses of copper and its alloys in structural, architecture, artistic, electrical, and electronic applications. Being negative to oxygen in the electromotive series but positive to hydrogen, copper can corrode only by oxygen reduction but not by hydrogen evolution from the electrochemical point of view.[3,4] The predominant cathodic reaction is the reduction of oxygen to form hydroxide ions:

$$O_2 + 2H_2O + 4e^- = 4OH^- \quad (1)$$

Anodically, the formation of Cu^{2+} ions is thermodynamically favored over the formation of Cu^+ ions:

$$2Cu = 2Cu^{2+} + 4e^- \quad (2)$$

However, if complexes are formed, e.g., depletion of Cu^+ by conversion to $CuCl_2^-$ in a chloride solutions, a univalent ion is the major dissolution product.[5]

Based on the above corrosion mechanism, it is easy to follow that (i) the coexisting of water and

* To whom correspondence should be addressed.

Journal of Applied Polymer Science, Vol. 60, 543–555 (1996)
© 1996 John Wiley & Sons, Inc. CCC 0021-8995/96/040543-13

oxygen or other oxidizing agents essentially cause the electrolyte corrosion process to take place; (ii) the presence of water is a key condition for the electrolyte corrosion processes that are possible; and (iii) the presence of ions accelerates the corrosion process.

Considerable research has been carried out to develop a "stainless copper," but the compositions so far developed have not met the stringent requirements for color and surface retention under service conditions. Corrosion protection methods currently employed include

1. The change of composition such as aluminum alloying of copper to improve oxidation resistance at high temperatures[6];
2. The change of the corrosive medium such as deaeration,[7] adding hydrate lime, caustic soda, soda ash, or a silicate to the copper plumbing systems[8];
3. Cathodic protection in the form of sacrificial magnesium, zinc anodes,[9,10] or sacrificial tin coating[11];
4. Applying passivation and corrosion inhibitors such as using benzotriazole (BTA) as both a liquid- and vapor-phase inhibitor[3-5,12]; and
5. Barrier coatings.[13]

However, some limitations are involved with each method: For instance, eliminating corrosive agents is not practical when copper is exposed to a large environment; efficient use of cathodic techniques is hampered by the lack of criteria for the requisite potential[10]; sacrificial tin coating may lead to failure due to non-pinhole free or ac-induced pit initiation mechanisms followed by autocatalytic pit growth in tin-coated copper neutral[11]; and the BTA inhibitor does not work in ammoniac atmosphere and solutions. Barrier coatings are effective because they keep moisture, oxygen, and other corrosive chemicals away from the metal substrate. Most conventional coating films, particularly paints and lacquers, however, permit chemicals, moisture vapor, and oxygen to permeate through them and attack the metal. Pinholes have a danger of causing pitting when a small anode area and a large cathode area is present.

Plasma polymerization, as a new coating technology for metal corrosion protection or passivation, has been explored since the 1960s. It should be realized that plasma polymerization is an ultrathin film technology. Therefore, the unique advantage of plasma polymerization is realized in ultrathin film applications (e.g., thickness of 100–5000 Å, particularly, the 100–500 Å).

It is well known that both barrier and adhesion properties of a protective layer are crucial in metal corrosion protection. Plasma polymers are generally formed in an extremely tight and three-dimensional network which behaves more like a low-permeability sieve than a solution–diffusion type of normal polymer. Because of this difference in the transport mechanism, it has been observed that the water-vapor permeability of an ultrathin layer of the plasma polymer (thickness around 200 Å) can be two to three orders of magnitude lower than that of polyethylene.[14] This is important considering the fact that the presence of moisture on the Cu surface is a key condition for the electrolyte corrosion process to take place. We are also aware, however, of the limitation due to the applicable thickness of plasma polymers (the barrier resistance is proportional to $\mathbf{l}/\mathbf{P}$, where $\mathbf{l}$ is the polymer film thickness, and $\mathbf{P}$, the permeability). It has been observed in our experiments[14] that the permeation lag time of water molecules through a 200 Å-thick plasma polymer [$\mathbf{P}$ in the scale of 10^{-14} cm^3_{STP} cm/cm^2 s (cmHg)] coated low-density polyethylene was only increased to about 4 or 5 h, comparable to 2.8 h of the virgin polyethylene substrate.

The destructive effect of water on adhesion can be seen in the often observed deterioration of dry adhesion strength by the influence of liquid- or vapor-phase water which surrounds the metal/polymer composite system. In the absence of a strong adhesion between polymer and the metal, the strong interaction of water molecules with both materials creates voids by delaminating polymer from the metal surface. In this way, macroscopic water clusters are able to develop at the interface and the metal surface is readily attacked. In this regard, the deposition of plasma polymers has the unique advantage that a water-insensitive interface can be formed so that the destructive influence of water molecules on the interface can be virtually eliminated by reason of the principle known as "atomic interfacial mixing" (AIM).[15]

In addition to the advantageous features already mentioned, another important feature with plasma polymer deposition is that surface cleaning and/or surface treatment can be applied directly before polymer deposition without breaking the vacuum. With good adhesion, *in situ* vacuum process characteristics, together with the excellent barrier characteristics of plasma polymers, plasma polymerization entitled itself to provide remarkable levels of corrosion protection of metal surfaces. In this study, plasma polymers of fluorocarbon, hydrocarbon, and organosilicones are deposited onto copper substrates. A wet/dry cycling test was adopted as an

accelerated copper corrosion testing method. The surface and interface region was examined by scanning electron microscopy (SEM) to characterize the adhesion conditions and failure mode.

EXPERIMENTAL

Materials

Copper specimens (1 × 1 × 0.02 in.) were used as substrates in this article. Prior to the start of each experiment, all the samples were washed in acetone using ultrasonic agitation to remove organic contaminant or dust from the surface, with part of them prepolished on SiC paper to 600 grid. After plasma polymer deposition, they were stored in a desiccator until the start of the corrosion exposure.

Three main categories of monomers were used as received to produce plasma polymerized (PP) coatings, namely:

1. organosilicones (trimethylsilane TMS [PCR] and hexamethyldisiloxane HMDSO [Aldrich Chemical]);
2. perfluorocarbons (perfluoroethane C_2F_6 [Matheson] and *n*-perfluorobutane C_4F_{10} [PCR]); and
3. hydrocarbon (methane CH_4 [Matheson]).

Plasma Polymerization

The dc (PlasmaCarb MPR-10R) and the af bell-jar reactor (PlasmaCarb MPR-500P) were described elsewhere.[14,16] For cathodic glow discharge polymerization, the two anode stainless-steel plates (10 × 10 × $\frac{1}{16}$ in.) were 6 in. apart. The copper samples were attached onto the cathode plate (4 × 6 in.) with silver paint which was placed halfway between the two parallel anodes. When anode magnetron glow discharge was carried out, eight permanent bar magnets were attached at the back side of each anode and were arranged in a spokelike configuration. The magnetic field strength of each magnet ranged from 700 to 800 Gauss. For af magnetron glow discharge polymerization, the copper samples were mounted on a rotating disk which is placed midway between aluminum electrodes with magnet bars placed uniformly at the back for uniform deposition.

An inductively coupled tubular reactor with a 13.56 MHz rf power source was used for plasma polymerization of HMDSO. The tubular reactor (132 cm long, 3.6 cm o.d., and 3.3 cm i.d.) with O-ring joints at both ends was made of Pyrex glass. Rf was sent through two ring-shaped electrode bands made of a thin copper sheet (1.3 cm wide, 8 cm long), which were fixed 6 cm apart on a wooden cart with four plastic wheels. The cart was able to move at a uniform axial rate along the reactor with an electric motor, speed controller, and chains.

Evaluation

The structure of coatings was characterized by various physicochemical techniques including Auger electron spectroscopy, electron spectroscopy for chemical analysis (ESCA), and scanning electron microscopy (SEM). In the present article, we deal primarily with SEM. The corrosion inhibition property was determined with the wet/dry cycle accelerating corrosion test.

Wet/Dry Cycle Accelerating Corrosion Testing

A Hotpack temperature–humidity chamber with adjustable temperature and humidity was used for this purpose. The process of corrosion is accelerated by increasing the relative humidity to 80% together with increasing temperature to 60°C and the concentration of chloride ions. Testing procedures are shown in Table I.

Visual Observation of Corrosion Attacks

Direct Visual Observation. Photographs of test samples were taken on a daily basis for the initial

Table I Wet/Dry Cycle Corrosion Test Using 0.1*N* NaCl Electrolyte[a]

1. Immerse coated copper samples in 0.1*N* NaCl solution for 15 min, then dry in air ventilating hood for 75 min
2. Transfer samples to the humidity chamber with constant RH and temperature at 80% and 60°C. The samples should be carefully placed so that no part of any samples is within 20 mm of another or within 100 mm of the walls or the ceiling. After being kept there for 20 h, they are moved out from the chamber
3. Rinse with distilled water thoroughly. The test will be continued with more cycles starting by immersing and drying each time. Carefully observe any change in copper samples from time to time; record the time when the first localized corrosion occurs as the induction time
4. If the samples have already been severely corroded, stop further testing
5. After 25 days, the cycle will be stopped and samples will undergo visual and SEM evaluation

[a] Based on ASTM B 380-65, B 368-68.

three cycles; later, photographs were taken every 3 days. This examination involves a qualitative statement of whether the metal has corroded or not. It is usually easy to see which type of corrosion occurs, if it is general corrosion or some type of local attack.

Scanning Electron Microscopy. Microscopic study is of particular value in examining deeply penetrating corrosion attacks, including pitting, cracking, crevice corrosion, etc. The SEM examination was carried out with a scanning electron microscope (Model 1600 turbo, Amray Inc., MA). It involved second electron analysis at 10 keV and 1000× magnification.

RESULTS AND DISCUSSION

Control Cu Surfaces

With copper, like many other metals, inorganic oxide films will normally form on storage in air. These films are quite passive and will slow down or prevent further deterioration of the metal. Micrographs of such a surface [Fig. 1(a)] showed a relative smooth surface containing a number of micropores. These micropores, under a wet/dry cycle corrosion test environment, render the underlying Cu to rapid pitting attack attributed to the large ratio of the cathodic area (copper oxide) to the anodic area (copper exposed at micropores or flaws) as shown in Figure 2(a).

In contrast, for those Cu specimens with the oxide layer removed, a rough surface from SiC polishing is illustrated in Figure 1(c), and after exposure, visual inspection revealed a considerable generalized attack with a layer of dark corrosion products fully covering the surface [Fig. 2(b)]. Under these conditions, the formation of a CuCl film of nonuniform thickness was reported.[17]

Plasma Polymer-coated Cu Surfaces

In view of limited passivation offered by Cu oxides, we studied the capacity of an ultrathin layer of plasma polymer coating in providing a protective and stable surface film able to withstand harsh chemical and thermal environments. Prior to exposure, the plasma polymer-coated surface was relatively smooth and featureless comparable to the uncoated surface, either unpolished or polished [Fig. 1(a) and (b) and Fig. 1(c) and (d)]. After exposure to the wet/dry cycle corrosion test, the surface was roughened to a various extent depending on the

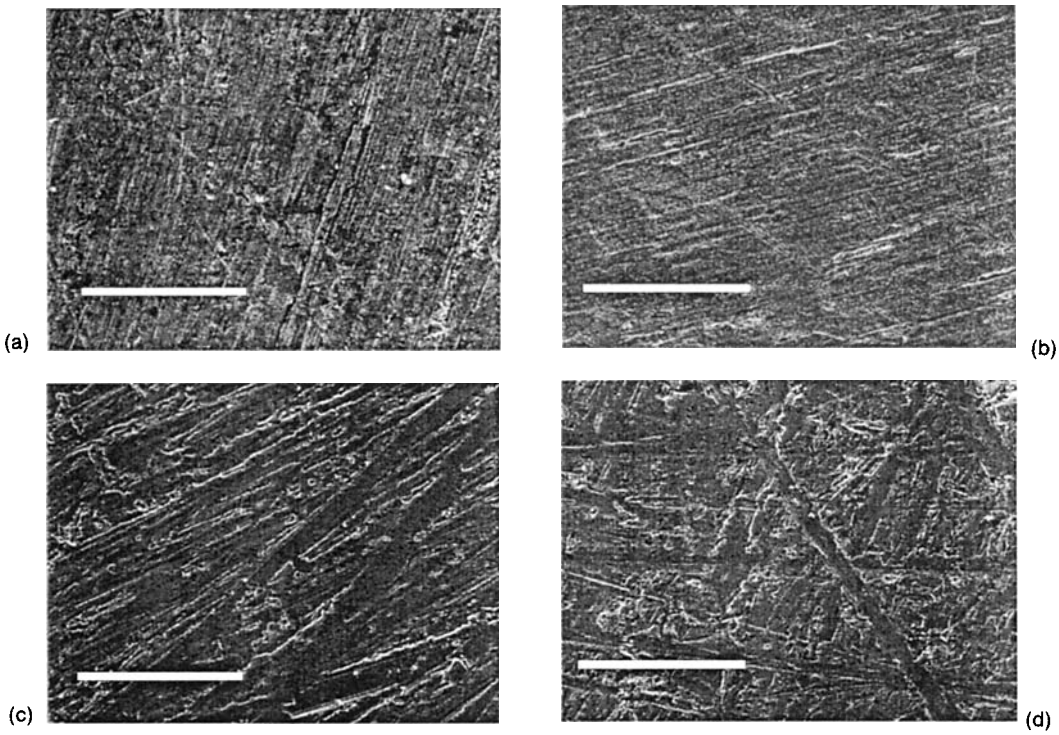

Figure 1 Scanning electron micrographs showing surface of copper: (a) unpolished Cu before plasma polymer deposition; (b) unpolished Cu after plasma polymer deposition; (c) polished Cu before plasma polymer deposition; (d) polished Cu after plasma polymer deposition (scale bars present 50 μm).

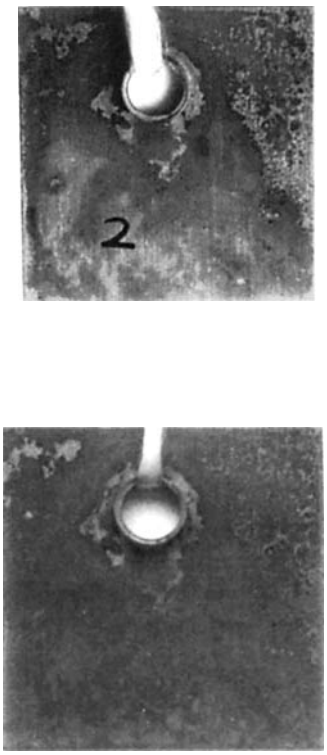

Figure 2 Visual appearance of bare copper after wet/dry cycle corrosion test: (a) unpolished bare copper; (b) polished bare copper.

plasma conditions. An underlying copper matrix was also observed in some cases.

In this study, no effect was made to measure the adhesive strength quantitatively. Instead, the wet adhesion strength was estimated from the ability to block local ruptures of the film and to restrict the expansion of the size of corroded area.

As noticed through the process of the exposure test, pitting or a localized attack was dominant. Protective film delamination or rupture appear to be caused by the forming of underlying corrosion products. After a pitting is initiated at the interface of the plasma polymer and Cu matrix, although a tendency toward filliform corrosion is possible, the volume of the corrosion product will try to stretch both vertically to rupture the protective layer and horizontally to delaminate or peel off the layer. When a strong wet adhesion is available, no expansion or only unsightly expansion of the size of the corrosion area occurred with the cycle test on. Accordingly, rupture dominated. Otherwise, quick expansion of the corrosion area on the surface is ready to occur and peel-off of the layer dominates.

The ability of plasma polymer coatings in Cu corrosion protection vary widely, depending on the details of the film preparation. A brief description of visual inspection together with the deposition parameters are listed in Table II–IV.

Cu/DC Cathodic Polymerization Coating System

The salient characteristic of the dc glow discharge is that the negative glow contains a higher concentration of ions, electrons, and other active species than does the positive column. The negative glow is also associated with an extensive bombardment of the cathode by high-energy ions. Accordingly, better adhesion can be achieved as a result of a greater interdiffusion between the plasma polymer and the metal substrate placed on the cathode, which undoubtedly contributes for the better corrosion protection. Preferential deposition of the plasma polymer on the cathode in a dc glow discharge has been reported.[18,19] Our research center's research projects indicates that cathodic polymerization seems the best glow discharge technique for metal substrate, such as cold-roll steel (CRS) plasma surface cleaning and polymerization to prevent it from corrosion.[16,20]

Without Magnetic Enhancement on Anode. In the absence of magnetic enhancement on the anode, methane cathodic polymerization-deposited surfaces (dc methane I) experienced a heavier corrosion attack [Fig. 3(a)]. The SEM observation showed the rupture of the protective layer and a clear localized attack of Cu leading to pitting [Fig. 4(a)]. Pitting indicated a nonuniform deposition which led to corrosion initiation at coating imperfections.

A comparable enhanced protective capacity was provided with TMS plasma coating prepared under lower system pressure (dc TMS I). Apart from a few pits, which were mounted with grayish corrosion products and randomly distributed over the surface, the rest of the surface remained shiny. Furthermore, the size of pitting was unsightly changed after 25 cycles of exposure. A well-refined rupture of the protective layer by the voluminous corrosion products surrounded by a smooth surface was also observed [Fig. 4(b)]. The nonexpansion of the pitting size and the clear boundary of the ruptured coating surface revealed a strong wet adhesion of this plasma polymer layer to the Cu oxide surface. A less protective film coating was observed when the system pressure was increased [Fig. 3(b)]. At the center of the attack, green patina was observed. The composition of green patina was described as $Cu_2(OH)_3Cl$.[11] The quick expansion of the pitting size from a tiny spot after two cycles of exposure to patches of corrosion indicated a very weak adhesive strength.

Table II Copper Corrosion Test of DC Cathodic Polymerization-coated Cu Specimens

Sample Group[a]	Wattage (W)	Flow Rate (sccm)	Time (min)	System Pressure (mTorr)	Induction Time (Cycle)	Degree of Protection and Surface Observations
Uncoated					1.00	No protection (generalized attack after 1 cycle)
No magnetic enhancement on anode						
Methane						
Dc methane I[b]	20.00	2.00	5.00	30.00	1.00	4 (pitting; black corrosion products randomly distributed all over the surface after 16 cycles)
TMS						
Dc TMS I[b]	25.00–3.00	2.00	2.00	30.00	3.00	3 (a few pits mounted with grayish corrosion products randomly distributed; the rest part of the surface remained shiny after 25 cycles)
Dc TMS II[c]	25.00–3.00	2.00	2.00	30.00	1.00	4 (generally attacked surface mounted with black corrosion products after 4 cycles)
Dc TMS III[b]	30.00–18.00	2.00	2.00	50.00	2.00	4 (patches of corrosion with green patina occupied at the center of black corrosion products after 4 cycles)
With magnetic enhancement on anode						
Methane						
Dc Methane II[b]	20.00	2.00	5.00	30.00	2.00	2 (superficial oxidation with easily wiped yellow power after 25 cycles)
Dc Methane III[c]	20.00	2.00	5.00	30.00	1.00	3 (patches of corrosion after 10 cycles)
TMS						
Dc TMS IV[b]	28.00–20.00	2.00	2.00	30.00		1 (only traces of tarnish at edges after 25 cycles)
Dc TMS V[c]	28.00–20.00	2.00	2.00	30.00		2 (a few randomly distributed black-colored pits; the rest of the surface remained shiny)

[a] All the Cu cubic samples are precleaned by ultrasonic for at least 0.5 h, then go through the wet/dry cycle accelerated corrosion tests.
[b] Unpolished Cu substrate surface.
[c] Polished Cu substrate surface (with SiC paper to 600 grid).

Dc Anode Magnetron Glow Discharge. When magnetrons were placed at the back of anode electrodes, corrosion of Cu surfaces was significantly suppressed. Anode magnetron glow discharge has recently been reported as a new plasma process used in plasma cleaning and polymerization.[21] One of the advantages of anode magnetron dc glow discharge over a non-anode-magnetron one is its ability to re-

Table III Copper Corrosion Test of AF Glow Discharge-coated Cu Specimens

Sample Group[a]	Wattage (W)	Flow Rate (sccm)	Time (min)	W/FM (MJ/kg)	System Pressure (mTorr)	Thickness (Å)[b]	Y[c]	Induction Time (Cycle)	Degree of Protection and Surface Observations
Uncoated								1.00	No protection (generalized attack after 1 cycle)
$C_4F_{10} + H_2$ (1 : 1)									
AF $C_4F_{10} + H_2$ I	8.50	4.75	11.00	19.97	150.00	83.00	2.30	2.00	2 (sparsely distributed tiny pits at edges after 25 cycles)
AF $C_4F_{10} + H_2$ II	12.00	3.88	4.00	34.57	150.00	53.00	2.00	1.00	3 (large black-colored patches of corrosion including pitting after 15 cycles)
$C_2F_6 + H_2$ (1 : 1)									
AF $C_2F_6 + H_2$ (1 : 1)	15.00	7.37		38.96	150.00	100.00		1.00	3 (small gray-colored patches of corrosion including pitting after 25 cycles)
CH_4									
Methane I	60.00	2.15	60.00	2,337.21	26.00	900.00	3.70	2.00	2 (sparsely distributed tiny pits at edges after 25 cycles)
Methane II	23.00	2.60	30.00	741.15	43.20	144.00	0.75	1.00	4 (large patches of corrosion)
	50.00	2.62	30.00	1,598.89	40.00	161.00			4 (large patches of corrosion)
Methane III	21.00	3.74		470.76	62.40	211.00	1.22	1.00	4 (large patches of corrosion)
	31.00	3.75		692.15	51.50	234.00		1.00	4 (large patches of corrosion)
	56.00	3.73	60.00	1,256.70	47.00	218.00		1.00	4 (large patches of corrosion)
Methane IV	39.00	4.85		673.59	83.60	303.00		1.00	3 (pits randomly distributed and mounted with black-colored corrosion products)
	65.00	4.87	60.00	1,118.73	63.80	353.00		1.00	3 (pits randomly distributed and mounted with black-colored corrosion products)
Methane V	59.00	5.93	45.00	833.26	80.50	537.00	1.62	1.00	2 (sparsely distributed tiny pits after 25 cycles)
	44.33	5.97	70.00	621.88	89.00	968.00		1.00	2 (a few randomly distributed pits)
	14.20	1.47	90.00	809.01	87.10	415.00		1.00	2 (tarnished surface after 25 cycles)

[a] All the Cu cubic samples are precleaned by ultrasonic for at least 0.5 h, then go through the wet/dry cycle accelerated corrosion tests.

[b] The thickness was read by a Rudolph ellipsometer on silicon wafers which were rotating with copper samples.

[c] Water vapor permeability reduction ratio given by ($P_{uncoated}/P_{coated}$).

Table IV Copper Corrosion Test of RF Glow Discharge-coated Cu Specimens

Sample No.[a]	Wattage (W)	Flow Rate (sccm)	Time (min)	W/FM (MJ/kg)	System Pressure (mTorr)	Thickness (Å)[b]	Induction Time (Cycle)	Degree of Protection and Surface Observations
Uncoated								No protection (generalized attack after 1 cycle)
TMS								
1	15.00	0.18	5.00	1,552.12	18.00	200.00	2.00	3 (several pits distributed at random after 15 cycles)
2	15.00	0.67	7.00	408.45	25.50	1,100.00	2.00	3 (several pits distributed at random after 15 cycles)
3	15.00	5.00	0.51	54.32	23.00	1,000.00	1.00	3 (small patches of corrosion after 5 cycles)
4	20.00	0.54	6.00	669.43	23.20	997.00	1.00	3 (several pits distributed at random after 15 cycles)
5	20.00	0.46	3.00	794.22	23.00	444.00	1.00	3 (tarnished at center of the surface; black patches of corrosion at edges after 5 cycles)

[a] All the Cu cubic samples are precleaned by ultrasonic for at least 0.5 h, then go through the wet/dry cycle accelerated corrosion tests.

[b] The thickness was read by a Rudolph ellipsometer on silicon wafers placed near copper samples.

duce the cathode sheath thickness in the low-pressure region. Thus, the negative glow gets closer to the cathode surface and a relatively larger proportion of high-energy ions reach the cathode, which makes a more effective plasma surface cleaning and polymer deposition comparable to nonmagnetron glow discharges in which the electron density N_e is higher at the edge region than in the center region of a cathode. Another advantage in a anode magnetron dc glow is that the negative glow is in a funnel-like shape on the interelectrode center adjacent to the anode electrode. The radial distributions of electron density N_e significantly peaked at the center of the radial position.[21] Accordingly, a more uniform deposition over the entire cathode surface can be achieved.

As shown in Figure 3(c), methane cathodic polymerization-coated Cu (dc methane II) showed only a superficial oxidation with a yellow layer of oxides easily removed. No noble corrosion took place and no penetrating pitting was seen. Superior corrosion protection was offered by the thin TMS cathodic polymerized film with anode magnetron enhancement (dc TMS IV). Figure 3(d) illustrates a shiny surface, albeit with a trace of grayish tarnish located at the edges. SEM examination of the edges revealed a partially detached and cracked protective layer at the tarnished spots [Fig. 4(c)], and some of the exposed Cu surface was roughened due to formation of oxidation products.

Deposition on Unpolished Cu Substrate Surface vs. on Polished Cu Substrate Surface. A general trend according to visual observation is that a plasma polymer film deposited on a polished Cu surface generally provides less protection than it did on an unpolished Cu surface. As described in Table II, a generalized attack was dominant on the polished surface while a pitting attack was dominant on the unpolished surface.

Without polishing, oxide film formed from storage was maintained. Chemical bonding was possibly formed between plasma polymers and Cu oxide, which contributes to an enhanced adhesion between plasma polymers and Cu substrates. Such a chemical bonding has been reported between organosilicon plasma polymers and metal oxides.[22] In the later stage of this study, all Cu specimens were used without SiC polishing.

Cu/AF and Cu/RF Glow Discharge Polymerization Systems

Perfluorocarbon Af Glow Discharge Deposited Coatings. After exposed to the wet/dry cycle corrosion test, visual inspection of the $C_4F_{10} + H_2$ (1 : 1) plasma-coated sample at lower-energy input il-

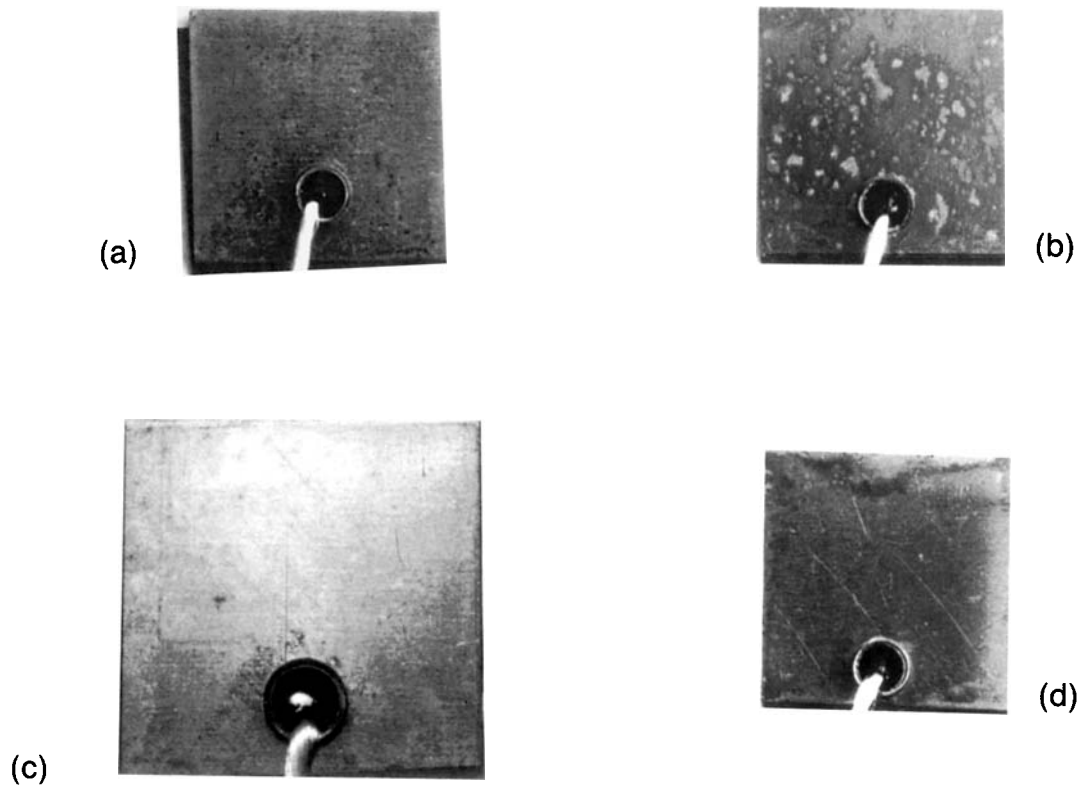

Figure 3 Visual appearance of Cu/dc cathodic glow discharge system after wet/dry cycle corrosion test: (a) methane I after 16 cycles; (b) TMS III after 4 cycles; (c) methane II after 25 cycles; (d) TMS IV after 25 cycles.

lustrated the presence of several pits sparsely distributed [Fig. 5(a)]. Micrographs showed that pits are shallow and the rest of the surface remained smooth. In contrast, as W/FM was increased, protection was much less effective. A generalized attack including pitting and dark corrosion products was observed [Fig. 5(b)].

The $C_2F_6 + H_2$ (1 : 1) plasma-coated surface revealed the formation of patches of light–dark corrosion products including pitting [Fig. 5(c)]. SEM examination revealed the formation of an island-structure porous film containing a number of small pores with amounts of corrosion products formed around them [Fig. 6(a)].

Methane Af Glow Discharge Deposited Coatings. In general, all methane plasma-coated Cu surfaces showed a certain density of pits distributed at random among either tarnished or a generalized attacked surface after two cycles of exposure. Five groups of plasma conditions were cataloged according to the deposition thickness. The effectiveness of the methane plasma-coated surface varies widely with the fabrication conditions and increase in the order of Groups II, III, IV < Group V < Group I.

After exposure, the methane plasma polymer coating under conditions in Group I provided a similar extent of anticorrosion protection as to that of the $C_4F_{10} + H_2$ (1 : 1) plasma-coated sample at a lower-energy input, as shown in Figure 5(d). In contrast, Cu surfaces prepared under Groups II–IV conditions showed either an overall (Group II) or partial coating (III and IV) of a thick layer of corrosion products [Fig. 5(f)]. The SEM picture in Figure 6(b) showed a compact and nearly uniform layer of a corrosion product coated over a surface prepared under Group II methane plasma polymerization. In addition, there is no evidence of penetrating pits. Cu surfaces of Group V, on the other hand, showed a typical localized attack of the metal [Fig. 5(e)].

TMS Rf Glow Discharge Deposited Coatings. A milder, less destructive discharge than af is attainable in rf glow discharge. The particular characteristics of an rf glow discharge is that the initiation and maintenance of electrons and ions which are necessary to sustain the glow takes place within the body of the plasma. This self-sustaining aspect of rf glow discharge makes use of an external electrode plausible and, thus, any contamination from the electrode material is eliminated.

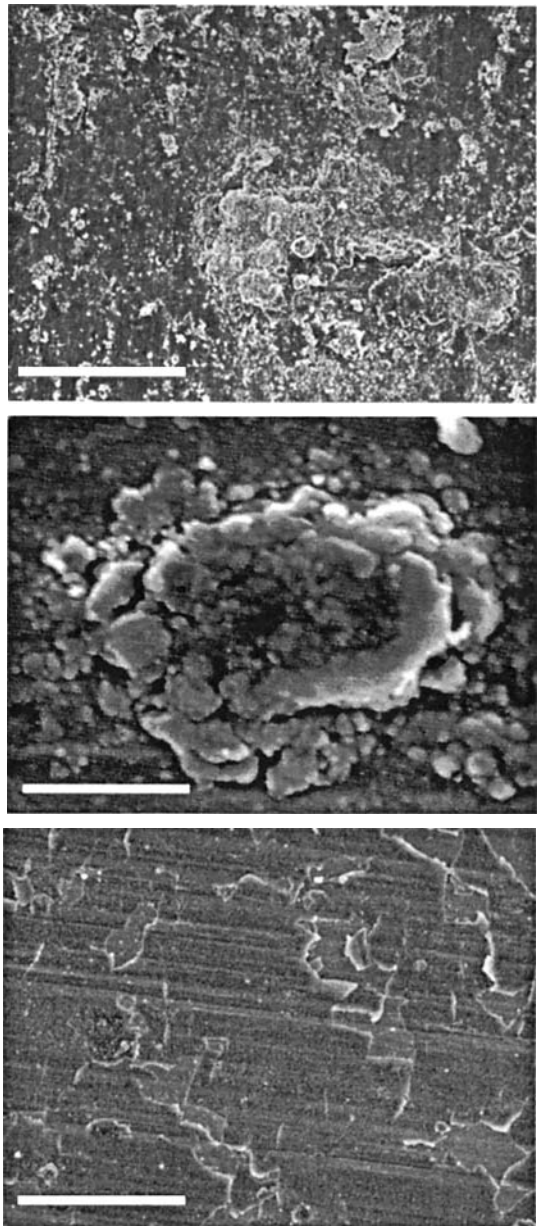

Figure 4 Scanning electron micrographs showing surface of Cu/dc cathodic glow discharge system after exposure: (a) methane I after 16 cycles; (b) TMS I after 25 cycles; (c) TMS IV after 25 cycles (scale bars present 50 μm).

The surface degradation of Cu specimens prepared by rf glow discharge occurred similarly to what happened on methane plasma-coated ones as shown in Figure 7(a) and (b). Nos. 1 and 2 Cu specimens were covered largely by a passivating layer with pits randomly distributed. A relatively smoother surface composed of tiny cracks and a detached area at pitting spots was observed [Fig. 6(c)]. The size of cracks and detached area increased for surfaces of nos. 3 and 4 Cu specimens as shown in Figure 6(d). Even though the surface was covered with a thin layer of the corrosion product, no penetrating pitting was observed on no. 5 Cu specimens.

Correlation Between Cu Corrosion Protection and Deposition Energy Input W/FM and Deposited Film Thickness

Comparing the anticorrosion capacity of glow discharge polymerized rf TMS 1 and rf TMS 2, it is not difficult to determine a very thin layer of film (20.0 nm) deposited for rf TMS 1 at the lowest flow rate, and, thus, the highest W/FM (1552.0 MJ/kg) led to a similar extent of anticorrosion capacity as to that of the film (rf TMS 2) which was deposited at a much lower energy level (408 MJ/kg) but a greater thickness (110 nm). In other words, both W/FM and the deposited film thickness play important roles in determining the Cu corrosion protection effectiveness of deposited plasma polymers.

W/FM Factor

The effect of W/FM on the anticorrosion performance of plasma polymers was closely related to its influence on the barrier and adhesion characteristics. The wet adhesive strength of plasma polymers has been reported to increase generally with energy input level, W/FM.[23,24] For example, Yasuda et al.[23] found that in order to achieve good water resistance adhesion of plasma-polymerized methane to platinum an energy level of exceeding 10^{10} J/kg is required. In a separate study,[24] Sharma and Yasuda investigated the wet adhesion of glow discharge polymerized tetramethyldisiloxane and its mixture with various ratios of oxygen to glass and platinum substrates. A clear indication was that the best water-resistant adhesion to both glass and platinum was obtained at the lowest monomer flow rate (F) and, thus, the highest-energy level W/FM.

The better adhesion characteristics of plasma polymers at higher-energy levels may be a consequence of higher crosslinkage of a plasma polymer and greater interdiffusion between plasma polymer and substrate (explained by the AIM principle).[23] Chemical bonding is also possible between plasma polymers and metal oxides.

The correlation of barrier properties with energy level depends on the monomer characteristics. For af glow discharge polymerized methane, the best water vapor permeation reduction ratio was obtained at the transient region (W/FM falls between 2000 and 2500 MJ/kg). TMS plasma polymers, on the other hand, did not offer any marked reduction in water vapor permeability under either af or rf glow

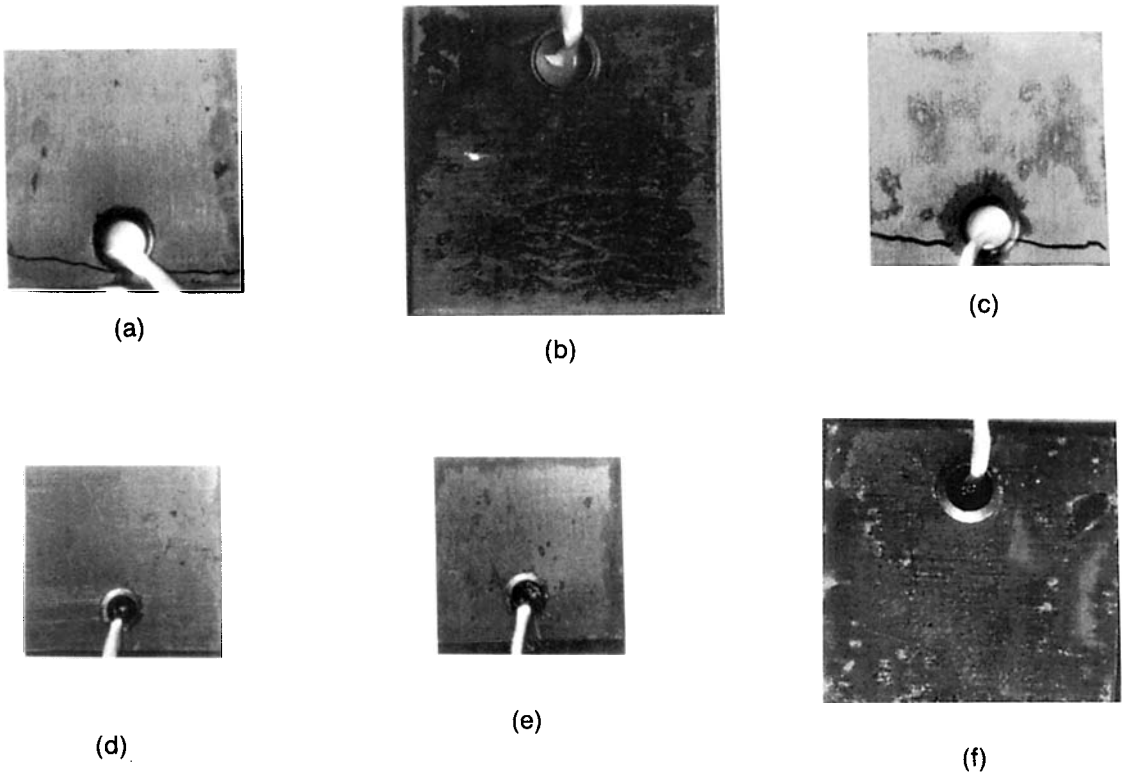

Figure 5 Visual appearance of Cu/af glow discharge system after wet/dry cycle corrosion test: (a) $C_4F_{10} + H_2$ (1 : 1) I after 25 cycles; (b) $C_4F_{10} + H_2$ (1 : 1) II after 15 cycles; (c) $C_2F_6 + H_2$ (1 : 1) after 25 cycles; (d) methane I after 25 cycles; (e) methane V after 15 cycles; (f) methane II after 3 cycles.

discharges over a broad range of energy level in this study.

Furthermore, a higher-energy level obtained with a lower flow rate rather than a higher wattage will increase the uniformity of the deposited film,[24] which has no doubt reduced the chance of pitting initiation. Accordingly, the superior Cu corrosion protection offered by the af methane I group comparable to af methane V was attributed to a higher-energy input, so that a strong wet adhesion, good water vapor permeation resistance, and a uniform coating [comparing Fig. 5(d) and (e)] was available. The superior Cu corrosion protection capacity of rf TMS 2 plasma polymer than that of rf TMS 3 was obviously due to the strong wet adhesion strength of the plasma and a uniform deposition.

Thickness Factor

As a rule of thumb, good adhesion of a relatively thick layer is more difficult to achieve than that of a very thin layer. However, it should also be noted that the film thickness should be greater than the minimum thickness required to cover the entire surface area of a substrate. As indicated in Table III, even though the energy level was increased by two to three times in each of the af methane II–IV groups, severe corrosion of the Cu surface occurred as a result of the noncomplete coverage of the Cu surface of methane plasma polymer layer. In summary, both high-energy input and complete surface coverage by a thicker film led to the optimum Cu corrosion protection of af methane I.

Correlation Between Anti-Cu Corrosion Performance and Water-Vapor Permeability of Plasma Polymer Coatings

Comparing the water-vapor permeability data listed in Table III and the corresponding results given by Figure 5(a) and (b) and Figure 5(d)–(f), it was found that within a series of plasma polymers, i.e., fluorocarbon plasma polymer or methane plasma polymer, a plasma polymer coating with higher water vapor transport resistance provided superior Cu corrosion protection. The accelerated electrical aging test with plasma polymer-coated LDPE samples revealed that the af $C_4F_{10} + H_2$ I plasma polymer showed a high efficiency in blocking the intrusion

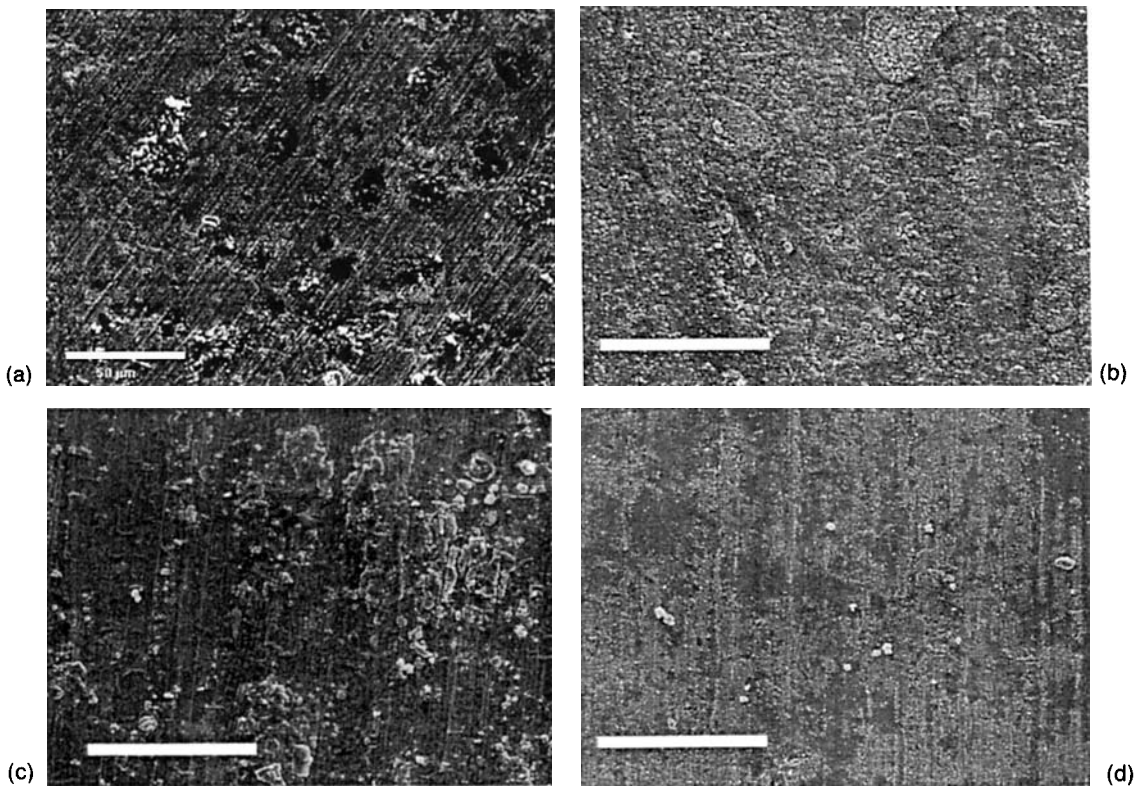

Figure 6 Scanning electron micrographs showing surface of Cu/af and Cu/rf glow discharge system after exposure: (a) af $C_2F_6 + H_2$ (1 : 1) after 25 cycles; (b) af methane II after 3 cycles; (c) rf TMS 1 after 15 cycles; (d) rf TMS after 3 cycles (scale bars present 50 μm).

of NaCl to the interface of plasma polymer and LDPE substrate. It has not been directly proved, however, whether a plasma polymer layer which offers better water vapor permeation resistance will provide superior ion intrusion resistance.

SUMMARY

Dc glow discharge of TMS with the anodic magnetron offers the best Cu corrosion protection due to the enhanced uniformity and tightness of the deposited plasma polymers. No corrosion was observed after 25 wet/dry cycle accelerated corrosion tests, while and uncoated Cu surface suffered a severe attack in one cycle. Superior corrosion protection was also performed by af plasma-polymerized coatings of $C_4F_{10} + H_2$ (1 : 1) at lower-energy input and of methane at high-energy input and with greater thickness within the range carried out in this study. The application of plasma polymers which had high water vapor permeation resistance and surface dynamic stability greatly reduced the pitting densities.

According to the extent of surface degradation after exposure, i.e., density of pits and depth of pits and size of corroded area, the protection ability of plasma polymer coatings was cataloged into the following four degrees:

1. Very effective. The surface remained shiny, and only a tiny trace of tarnish due to the partial detachment of the protective layer led to oxidation of the exposed copper matrix, such as the dc anode magnetron glow discharge-coated Cu surface at a low system pressure with the TMS monomer (dc TMS IV).
2. Effective. Most of the surface remained shiny, albeit with few nonpenetrating pits sparsely distributed, such as dc methane II, af $C_2F_{10} + H_2$ (1 : 1) I, and af methane I.
3. Modest. Typical localized attack with pits randomly distributed on slightly tarnished surface. The attacked layer appeared cracked and partially detached, such as af methane V, rf TMS 1 and 2, and dc TMS I.
4. Little. The surface showed a generalized attack including pittings and films assigned to corrosion products.

(a)

(b)

Figure 7 Visual appearance of Cu/rf glow discharge system after wet/dry cycle corrosion test: (a) TMS 1–15 cycles; (b) TMS 5–5 cycles.

This study was supported partially by a National Science Foundation Grant, NSF CTS 9101723, and is here gratefully acknowledged.

REFERENCES

1. A. R. Westwood, *Eur. Polym. J.*, **7**(4), 363 (1971).
2. T. Wang and H. Yasuda, *J. Appl. Polym. Sci.*, to appear.
3. S. Sankarapavinasam and M. F. Ahmed, *J. Appl. Electrochem.*, **22,** 390–395 (1992).
4. C. Clerc and R. Alkire, *J. Electrochem. Soc.*, **138**(1), 25–33 (1991).
5. G. Xue and J. Ding, *Appl. Surf. Sci.*, **40,** 327–332 (1990).
6. K. T. Chiang, K. J. Kallenborn, and J. L. Yuen, *Surf. Coat. Technol.*, **52,** 135–139 (1992).
7. M. B. McNeil, A. L. Amos, and T. L. Woods, *Corrosion,* **49**(9), 755–758 (1993).
8. A. Cohen and J. R. Myers, *Mater. Perform.*, **Aug.,** 43–45 (1993).
9. H. L. van Heugten, *Mater. Perform.*, **Apr.,** 48–51 (1991).
10. EPRI Research Project, RP 1049-01, EL-1970, V.1, Aug., 1981, 178 pp.
11. O. J. Van Der Schijff and O. F. Devereux, *Corrosion,* **49**(4), 310–314 (1993).
12. V. Brusic, M. A. Frisch, B. N. Eldridge, F. P. Novak, F. B. Kaufman, B. M. Rush, and G. S. Frankel, *J. Electrochem. Soc.*, **138**(8), 2253–2258 (1991).
13. J. Jang and H. Ishida, *Corros. Sci.*, **33**(7), 1053–1066 (1992).
14. Y. Lin, PhD Dissertation, University of Missouri-Columbia, 1995.
15. H. Yasuda, *Plasma Polymerization,* Academic Press, New York, 1985.
16. T. H. Wang, PhD Thesis, University of Missouri-Columbia, May 1994.
17. M. R. G. de Chialvo, R. C. Salvarezza, D. Vasquez Moll, and A. J. Arvia, *Electrochem. Acta,* **30,** 1501 (1985).
18. N. Morosoff, W. Newton, and H. Yasuda, *J. Vac. Sci. Technol.*, **15**(6), 1815–1822 (1978).
19. H. U. Poll, M. Arzt, and K. H. Wickleder, *Eur. Polym. J.*, **12,** 505 (1976).
20. B. H. Chun, PhD Thesis, University of Missouri-Columbia, May, 1994.
21. W. H. Tao, PhD Thesis, University of Missouri-Columbia, August, 1994.
22. A. K. Hays, *Thin Solid Films,* **84,** 401 (1981).
23. H. Yasuda, A. K. Sharma, E. B. Hale, and W. J. James, *J. Adhes.*, **13,** 269 (1982).
24. A. K. Sharma and H. Yasuda, *Thin Solid Films,* **110,** 171 (1983).

Received September 19, 1995
Accepted October 13, 1995